Int. Journal of Refractory Metals and Hard Materials 53 (2015) 80–86

Contents lists available at ScienceDirect

Int. Journal of Refractory Metals and Hard Materials

journal homepage: www.elsevier.com/locate/IJRMHM

Activated liquid phase sintering of W–Cu and Mo–Cu

John L. Johnson

Elmet Technologies LLC, 1560 Lisbon St., Lewiston, ME 04240, United States

ARTICLE INFO

Article history:
Received 31 January 2015
Received in revised form 16 March 2015
Accepted 27 April 2015
Available online 29 April 2015

Keywords:
Tungsten
Molybdenum
Tungsten–copper
Molybdenum–copper
Liquid-phase sintering
Grain growth

ABSTRACT

A model for densification based on the master sintering curve concept is applied to solid-state sintering of W and Mo and to liquid-phase sintering of W–10Cu and Mo–18Cu. The effects of small additions of Ni, Co, Fe, and Pd to W–10Cu and Mo–18Cu are investigated. Separate grain growth models for solid-state and liquid-phase sintering are also applied to these systems. The model predictions are compared to experimental results to determine the effects of the activators on densification and grain growth mechanisms. Ni and Pd additions only slightly reduce the activation energy for densification, while Co and Fe have a much larger effect. The effects of Co and Fe additions on grain growth rate constants are not adequately described by consideration of their effects on the solubility of W and Mo in the liquid phase. The experimental results with Co and Fe additions are better described by a solid-state grain growth model. The effects of Co and Fe additions on densification and grain growth are consistent with enhanced diffusion through a segregated solid phase during liquid-phase sintering.

1. Introduction

The high diffusion rates of liquid phases can provide rapid densification and grain growth during sintering. In classic systems, such as W–Ni–Cu and W–Ni–Fe alloys, the liquid phase that forms has substantial solubility for the base solid phase, resulting in dissolution of small particles and convex surface features [1]. The dissolved base phase then reprecipitates on larger particles and concave surfaces resulting in grain spheroidization and coarsening. Porosity is virtually eliminated.

Liquid-phase sintering of systems such as W–Cu and Mo–Cu, in which the base metal has little solubility in the liquid phase, results in poor densification behavior and slow grain growth rates. Submicrometer W particle sizes are needed to sinter W–Cu to near full density [2–4], while full density for Mo–Cu requires Mo particle sizes less than about 2 μm [2,5–9]. Sintered grains are not much larger than the starting particle size.

For W–Cu, the solubility of W in Cu is less than 10^{-3} at.% [10], and grain growth likely occurs by a combination of solution-reprecipitation [11–13] and coalescence [14–16]. For Mo–Cu the reported solubility of Mo in Cu of 0.5 to 1.3 wt.% at 1100 to 1500 °C [17] would be expected to result in a dominant role for solution-reprecipitation, but reported grain growth rates are much lower, raising the probability of a significant contribution from coalescence [18].

Substituting small amounts of other transition metals for Cu can significantly increase the solubility of W and Mo in the liquid phase. Ni and Pd are completely soluble in Cu and substituting 1 wt.% Ni for Cu increases the W solubility by more than an order of magnitude [16]. This increase in solubility improves densification behavior, but Co and Fe are more effective than Ni at enhancing densification of W–Cu [19–21]. Co and Fe have similar solubility for W, but are less soluble in Cu so they segregate to the surfaces of W grains [22] where they are more effective in small quantities by activating solid-state sintering of the W skeleton.

New analytical methods based on the master sintering curve (MSC) concept enable further analysis of the densification kinetics of these systems to provide an improved understanding of the sintering mechanisms involved in “activated” liquid-phase sintering. Initially developed by Su and Johnson [23] to obtain a single apparent activation energy for densification of a given ceramic system, the MSC equations were modified by Park et al. [24,25] to calculate apparent activation energies for both densification and grain growth for W–Ni–Fe alloys before, during, and after formation of the liquid phase. These modified MSC equations were further used to calculate the apparent activation energy for sintering, densification function, and work of sintering for W–Ni–Fe, W–Ni–Cu, and W–Cu to create a master sintering surface for different solubilities of W in the liquid phase [26].

In this paper, a model for densification based on the MSC concept is applied to solid-state sintering of W and Mo and to liquid-phase sintering of W–Cu and Mo–Cu. The effects of small additions of Ni, Co, Fe, and Pd for Cu are investigated. Separate grain growth models for solid-state and liquid-phase sintering are also applied to these systems. The model predictions are compared to experimental results to determine the effects of the activators on apparent activation energies for densification and grain growth rate constants.

http://dx.doi.org/10.1016/j.ijrmhm.2015.04.030
0263-4368/

Table 1
Characteristics of the W, Mo, and Cu powders.

Powder	W	W	W	W	Mo	Mo	Cu	Cu
Vendor	Firth Sterling	GTP	Firth Sterling	GTP	Climax	Climax	ACuPowder	ACuPowder
Designation	C-3	M10	C-5	M35	012293	102792	2000	635
Particle size distribution								
D_{10} (μm)	0.6	0.9	1.8	2.7	1.1	2.1	1.3	8.2
D_{50} (μm)	1.5	2.1	5.1	6.2	2.5	4.1	3.6	12.5
D_{90} (μm)	10.0	7.2	16.4	14.2	4.8	7.9	5.5	19.2
BET particle size (μm)	0.11	0.23	0.49	1.08	0.47	1.52	1.80	5.71
Pycnometer density (g/cm^3)	18.4	18.4	19.0	18.4	9.62	10.14	8.78	8.8
Apparent density (g/cm^3)	2.0	1.9	2.6	2.8	2.1	3.0	3.3	3.3
% of pycnometer density	11%	10%	14%	15%	21%	29%	38%	38%
Tap density (g/cm^3)	3.2	3.7	3.2	5.0	3.1	5.0	3.7	3.8
% of pycnometer density	17%	20%	24%	27%	31%	49%	42%	43%

2. Models

2.1. Densification

The dependence of the fractional apparent density ρ_A on the particle size can be expressed as follows [27,28]

$$\log\rho_A = \log\rho_0 + a\log D \qquad (1)$$

where ρ_0 is the fractional packing density of a 1 μm powder, a is a constant, and D is the median particle size in μm. Prior work [29] determined values of 0.206 and 0.070 for ρ_0 and a, respectively, for W powders with D given by the BET particle size in μm.

The fractional green density ρ_g has been linked to the particle size and compaction pressure by the following empirical equation [29]

$$\rho_g = 1+\rho_A\left(1-\exp\left(\frac{A}{D^{1/7}}-\frac{P^{1/2}}{C}+E\right)\right) \qquad (2)$$

where A relates to particle rearrangement behavior, ρ_A is the fractional apparent density, D is the BET particle size, P is the compaction pressure, C relates to material strength, and E is a constant. Prior work [29] determined vales of 0.608 for A, 73.8 for C, and 0.735 for E with D in μm and P in MPa for W. These values were also used for Mo in the present work since they provided a better fit to the data than the values of 1.529 for A, 36.1 for C, and 0 for E previously determined for Mo [29]. To approximate the experimental green densities, a fixed green density of 0.55 was used for W–Cu and Mo–Cu.

The sintered density depends on the green density ρ_g and the linear sintering shrinkage $\Delta L/L_g$ according to

$$\rho_s = \frac{\rho_g}{\left(1-\frac{\Delta L}{L_g}\right)^3}. \qquad (3)$$

The sintering shrinkage displays an asymptotic character as the compact nears full density. The MSC approach [23] accounts for this behavior, which can be represented by a sigmoid function as given by the following relation [27,28]

$$\frac{\Delta L}{L_g} = f_1 + \frac{f_2}{1+\exp\left(\frac{f_3-Y}{f_4}\right)} \qquad (4)$$

where $f_1 = 0.01$, $f_2 = 0.165$, $f_3 = 0.104$, and $f_4 = 0.015$, and Y is a densification factor that can be calculated from an Arrhenius-type equation as follows:

$$Y = \frac{1}{D^v}\exp\left(B_S t^w - \frac{Q}{RT}\right) \qquad (5)$$

where D is the particle size, w and v depend on the diffusion mechanism, B_S is a material parameter, t is the sintering time, Q is the activation energy for densification, R is the gas constant, and T is the sintering temperature. From previous work [27,28], $B_S = 0.0054$, $Q = 30.4$ kJ/mol, $v = 0.444$, and $w = 0.119$ when the W particle size D is in μm and time t is in minutes. Other work [29] found $Q = 36.0$ kJ/mol best fit experimental data for sintering temperatures ranging from 900 to 1200 °C using the BET particle size for D. The activation energy was treated as an adjustable parameter for the material systems investigated in the present work.

2.2. Grain growth

For solid-state sintering, the mean grain size G_m depends on sintering temperature, hold time, initial grain size, and the effects from porosity and pore drag as follows [27,28]:

$$G_m - G_o = K' t^{1/n}\left(\frac{\rho_g}{1-\rho_s}\right)^{1/2}\exp\left(\frac{-Q_G}{RT}\right) \qquad (6)$$

where G_o is the initial particle size, K' is a collection of material constants, t is the isothermal time at absolute temperature T, n is a constant that depends on the grain growth mechanism, ρ_g is the fractional green density, ρ_s is the fractional sintered density, and Q_G is the activation energy for grain growth. For W, $K' = 23.5$ μm/s$^{1/3}$, $n = 3$, and $Q_G = 86$ kJ/mol when the particle size G_o is in μm and time t is in seconds [29].

For liquid-phase sintering, the mean grain size G_m obeys the following relationship [30]:

$$G_m^n - G_o^n = Kt \qquad (7)$$

where G_0 is the initial grain size, K is the grain growth rate constant, t is the time, and n is the growth rate exponent. The growth rate exponent

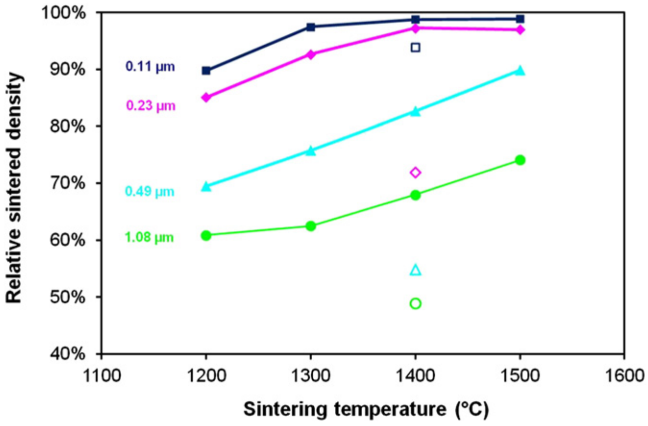

Fig. 1. Effect of sintering temperature and W particle size on the density of W (open markers) and W–10Cu (solid markers) after compacting at 70 MPa and sintering for 1 h in hydrogen.